Journal of Neuroscience Methods 189 (2010) 216–229

Contents lists available at ScienceDirect

Journal of Neuroscience Methods

journal homepage: www.elsevier.com/locate/jneumeth

Short and long term biocompatibility of NeuroProbes silicon probes

László Grand[a,b,c], Lucia Wittner[a,c], Stanislav Herwik[d], Emmanuelle Göthelid[e], Patrick Ruther[d], Sven Oscarsson[e], Hercules Neves[f], Balázs Dombovári[a,b,d], Richárd Csercsa[a,b,d], György Karmos[b], István Ulbert[a,b,*]

[a] Institute for Psychology, Hungarian Academy of Sciences, Budapest, Hungary
[b] Péter Pázmány Catholic University, Faculty of Information Technology, Budapest, Hungary
[c] Institute of Experimental Medicine, Hungarian Academy of Sciences, Budapest, Hungary
[d] Department of Microsystems Engineering (IMTEK), University of Freiburg, Freiburg, Germany
[e] Department of Physics and Astronomy, Uppsala University, Uppsala, Sweden
[f] Interuniversity Microelectronics Centre (IMEC), Leuven, Belgium

ARTICLE INFO

Article history:
Received 6 January 2010
Received in revised form 12 March 2010
Accepted 8 April 2010

Keywords:
Silicon probes
Rat neocortex
Neuron density
Glial reaction
Surface treatment

ABSTRACT

Brain implants provide exceptional tools to understand and restore cerebral functions. The utility of these devices depends crucially on their biocompatibility and long term viability. We addressed these points by implanting non-functional, NeuroProbes silicon probes, without or with hyaluronic acid (Hya), dextran (Dex), dexamethasone (DexM), Hya + DexM coating, into rat neocortex. Light and transmission electron microscopy were used to investigate neuronal survival and glial response. The surface of explanted probes was examined in the scanning electron microscope. We show that blood vessel disruption during implantation could induce considerable tissue damage. If, however, probes could be inserted without major bleeding, light microscopical evidence of damage to surrounding neocortical tissue was much reduced. At distances less than 100 μm from the probe track a considerable neuron loss (~40%) occurred at short survival times, while the neuronal numbers recovered close to control levels at longer survival. Slight gliosis was observed at both short and long term survivals. Electron microscopy showed neuronal cell bodies and synapses close (<10 μm) to the probe track when bleeding could be avoided. The explanted probes were usually partly covered by tissue residue containing cells with different morphology. Our data suggest that NeuroProbes silicon probes are highly biocompatible. If major blood vessel disruption can be avoided, the low neuronal cell loss and gliosis should provide good recording and stimulating results with future functional probes. We found that different bioactive molecule coatings had small differential effects on neural cell numbers and gliosis, with optimal results achieved using the DexM coated probes.

1. Introduction

Recent neocortical prostheses begin to offer exceptional possibilities for restoring cerebral function (Schwartz, 2004). Furthermore, multiple microprobes for cerebral recording and stimulation are vital tools to advance understanding of cellular and systems level function in the central nervous system. While significant success has been achieved with these approaches, the interface between brain tissue and implanted prostheses or probes can still be greatly improved. Important aspects of this interface include: (1) reaching neurons at the desired location in the brain; (2) ensuring consistent electrical recording and stimulation conditions in the long term; and (3) rendering the devices as inert as possible in terms of biocompatibility, biostability and biofouling.

The European Project NeuroProbes (http://www.neuroprobes.eu) aims to achieve an optimal neural tissue-probe interface. Single and multiple shank silicon-based NeuroProbes microprobes are developed and combined with chemical sensors and microfluidic systems (Frey et al., 2007; Neves et al., 2007; Ruther et al., 2008; Spieth et al., 2008). The specific microsystem integration of NeuroProbes is designed so that these features can be integrated into a common platform in a modular fashion (Aarts et al., 2008). This will permit a consistent and combined use of biosensors, drug delivery paths, electrical recording and stimulation to understand brain function.

* Corresponding author at: Institute for Psychology, Hungarian Academy of Sciences, 1068 Budapest, Szondi u. 83-85, Hungary, Tel.: +36 1 354 2395; fax: +36 1 354 2416.
E-mail address: ulbert@cogpsyphy.hu (I. Ulbert).

0165-0270/$ – see front matter © 2010 Elsevier B.V. All rights reserved.
doi:10.1016/j.jneumeth.2010.04.009

Long term viability and biocompatibility is a key attribute of implanted microprobes. Even materials considered to be biocompatible can induce adverse brain reactions. Two major factors determine the degree of tissue response. First, when a probe is inserted, it causes mechanical damage, damaging brain cells, disrupting blood vessels and thus compromising the blood–brain barrier. Second, an inflammatory neural tissue reaction is induced by both the implant and the injury it causes (for review see Cheung, 2007). This usually results in the development of a glial scar around the probe, which tends to reduce the efficacy of neuronal recording and stimulation (Edell et al., 1992; Fawcett and Asher, 1999; Polikov et al., 2005; Schwartz, 2004; Shain et al., 2003; Szarowski et al., 2003; Turner et al., 1999).

Probes are usually implanted for long term recordings lasting weeks or months. Therefore they should not be susceptible to attack by biological fluids, proteases, macrophages, brain metabolic factors. Silicon seems to be a good candidate as resistant material for long term recording probes. Surface damage is usually reported if stimulation has been performed through the electrodes of the probe (for review see Merrill et al., 2005). At the same time, scanning electron microscopy shows adherent cells and tissue residue on the surface of the explanted probes (Biran et al., 2005; Hoogerwerf and Wise, 1994; Turner et al., 1999).

Within the NeuroProbes project, we emphasize long term chronic use of the silicon microprobes and seek actively to diminish inflammatory and glial responses to implantation. The silicon surface of the probes was coated by different molecules, in order to produce more biocompatible surfaces for use in brain implants. We followed three main directions. First, we attempted to create a surface resembling the habitual environment of the neural tissue using hyaluronic acid (Hya) coating. Hya is a naturally occurring polysaccharide, which forms an important component of the extracellular matrix (Fraser et al., 1997). In addition, Hya has an important role in biological processes such as cell motility, cell differentiation and wound healing (Pasqui et al., 2007; Pouyani and Prestwich, 1994). Injecting hyaluronic acid into an injured area was shown to reduce glial scar formation in the rat neocortex (Lin et al., 2009). Second, we aimed to decrease bleeding due to mechanical damage by coating probes with dextran (Dex). Dex is a complex polysaccharide, used medicinally as an antithrombotic agent to reduce blood viscosity and vascular thrombosis (Gallus and Hirsh, 1976). It binds erythrocytes, platelets, and vascular endothelium, so reducing erythrocyte aggregation and platelet adhesiveness (for reviews see Abir et al., 2004; Johnson and Barker, 1992). Clots formed in the presence of Dex are more easily lysed due to an enhanced fibrinolysis (Jones et al., 2008). Furthermore, surface immobilized Dex limits cell adhesion and spreading (Massia et al., 2000). Thirdly we attempted to reduce tissue reaction by coating probes with the anti-inflammatory drug dexamethasone (DexM). DexM is a synthetic and potent steroid hormone of the glucocorticoid class. Systemic DexM administration attenuates glial responses in rat neocortex (Shain et al., 2003; Spataro et al., 2005), but may also have serious side effects (Kaal and Vecht, 2004; Koehler, 1995; Twycross, 1994). Previous work suggests that implanted silicon probes coated with DexM reduces the tissue reaction and lowers neuronal loss (Zhong and Bellamkonda, 2007; Zhong et al., 2005).

Here we used several microscopical methods to quantify short and long term neuron loss and glial reaction in response to the implantation into rat neocortex of NeuroProbes silicon probes. Light and transmission electron microscopy, as well as stereological methods were used to examine cellular responses and scanning electron microscopy was used to reveal the modifications of the probe surface caused by the brain tissue. The effect on the tissue reaction of different coatings, including Hya, Dex, DexM and Hya/DexM, was investigated.

2. Methods

2.1. Probe implantation and explantation

The biocompatibility of NeuroProbes silicon probes was tested in vivo, in the neocortex of Wistar rats ($n = 13$). All implanted multiple microprobe had four, 2-mm-long shanks, and were non-functional, i.e. were not equipped with output cables. Three different types of probes were implanted (Fig. 1, Table 1). (1) E100P probes had shanks with a cross section of 140 μm × 100 μm at the connector part gradually decreasing to 100 μm × 100 μm close to the tip, with an opening angle of 17°, five Pt electrode contacts (20 μm diameter, and 400 μm distance between contacts) on each shank, and a thin probe base for platform-based assembly (thickness is 300 μm, with four segments of 400 μm × 300 μm, E100P = Electrode, 100 μm, Platform assembly; details on platform assembly given in Aarts et al., 2008). (2) D100C probes had the same shank size as E100P probes but no Pt contacts on the shafts, and a wider probe base for cable assembly (thickness 300 μm, dimensions 2440 μm × 640 μm, D100C = Dummy, 100 μm, Cable assembly; Herwik et al., 2009). (3) D150C probes had shanks of 150 μm × 100 μm at the tip, no Pt contacts, and the wide probe base for cable assembly (D150C = Dummy, 150 μm, Cable assembly; Table 1, Fig. 1). The fabrication process of these silicon-based probes is detailed in (Herwik et al., 2009).

The effect of four different coatings was tested. Five probes – of the same type – were implanted in each rat, one without coating (Si), and four with coatings of hyaluronic acid (Hya), dextrane (Dex), dexamethasone (DexM) or a mixture of hyaluronic acid and dexamethasone (Hya/DexM). Two probes (Si, Hya) were implanted in one cortical hemisphere, and three (Dex, DexM, Hya/DexM) into the other. All implantations were made in dorsal neocortical areas between bregma and lambda (Paxinos and Watson, 1998). Surgery was performed under ketamine/xylazine anesthesia (ketamine: 75 mg/kg, xylazine: 5 mg/kg) and consisted of making independent craniotomies for the 5 probes in each rat. The probes were implanted by hand with a fine forceps, through the intact dura. The extradural superstructure was than embedded into dental acrylic, which was in turn anchored to the bone, thus the probe was tethered to the skull. After implantation, the skin was sutured back.

After fixation of the brain, (see below) explantation of the probes was performed manually by grinding away the cranium at the edge of the dental acrylic implant and carefully pulling out the fixed brain by hand. For an experienced histologist, post-fixation damage is clearly distinguishable from damage originated from the living tissue, thus we were able to exclude any post-fixation artifacts from our analysis.

2.2. Coating procedure

The coatings were performed after functionalization of both the molecules and the probes in order to allow the covalent bonding of the former onto the later. Thiol groups were introduced onto the probes surfaces through silanisation (Ledung et al., 2001). The thus functionalized probes were then immersed in pyridine-disulfide substituted Hya and Dex, which then reacted with the thiol groups introduced on the surface. The procedure was slightly different for dexamethasone, where the thiopyridine groups were introduced already on the silinised probe surface (Ledung et al., 2001), and could then react with the thiol substituted anti-inflammatory molecule.

2.3. Histology

Animals were sacrificed at 1 week ($n = 3$ animals), 2 weeks ($n = 3$), 4 weeks ($n = 3$), 8 weeks ($n = 1$) and 12 weeks ($n = 3$) after

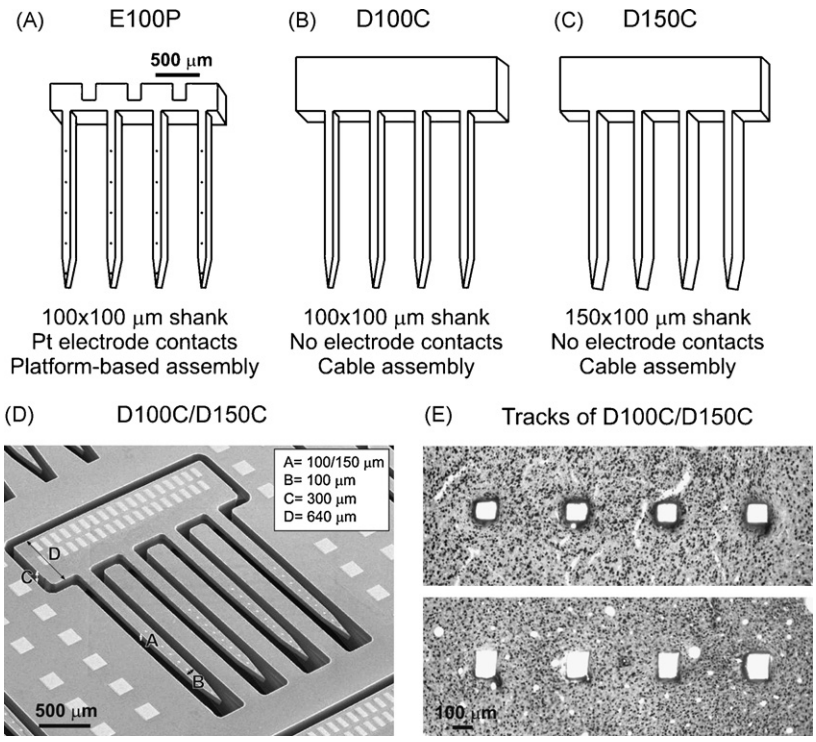

Fig. 1. Schematic drawing of implanted probe types (see details in Herwik et al., 2009). Probes E100P had shanks with a cross section of 100 μm × 100 μm at the tip, five Pt electrode contacts on each shank, and a thin probe base for platform-based assembly (A). Probes D100C had shanks of 100 μm × 100 μm, no electrode contacts on the shafts, and a wider, 300 μm thick probe base for cable assembly (B). Probes D150C had shanks of 150 μm × 100 μm, no electrode contacts, and the wide probe base for cable assembly (C). A scanning electron micrograph shows a D100C probe in the silicon wafer (D). Size of the probes are indicated. Tracks of D100C and D150C probes are compared on light micrographs from the neuronal marker NeuN-stained sections (E).

probe implantation (Table 1). They were perfused through the heart with physiological saline followed by a fixative containing 4% paraformaldehyde with 15% saturated picric acid in 0.1 M phosphate buffer (PB). Probes were explanted and stored in the same fixative for processing. The brain was removed from the skull, and postfixed in the same solution at 4 °C, overnight. Horizontal sections (60 μm thick) were cut with a Vibratome, washed with PB, and freeze-thawed above liquid N_2 in 0.1 M PB containing 30% sucrose. Endogenous peroxidase activity was blocked with 1% H_2O_2. Non-specific staining was suppressed with 5% skim milk powder and 2% bovine serum albumin in 0.1 M PB. Monoclonal mouse antibodies were used against the neuronal marker NeuN (1:3000, Chemicon, Temecula, CA, USA) and the glial fibrillary acidic protein GFAP (1:5000, Novocastra, Newcastle upon Tyne, UK) for 24 h at 4 °C. The specificity of the antibody was tested by the manufacturer. Immunopositive elements were visualized using biotinylated anti-mouse immunoglobulin G (1:300, Vector, Burlingame, CA, USA) as a secondary antiserum followed by avidin-biotinylated horseradish peroxidase complex (ABC; 1:300, Vector, Burlingame, CA, USA). The immunoperoxidase reaction was developed using 3,3′-diaminobenzidine tetrahydrochloride (DAB; Sigma, St Louis, MO, USA) dissolved in Tris buffer (TB, pH 7.6) as a chromogen. Sections were osmicated (20 min, 0.5% OsO_4), dehydrated in ethanol, and mounted in Durcupan (ACM; Fluka, Buchs, Switzerland).

2.4. Electron microscopy

2.4.1. Transmission electron microscopy

After light microscopic examination, areas of interest were re-embedded and sectioned for electron microscopy. Ultrathin serial sections were collected on Formvar-coated single slot grids, stained with lead citrate, and examined with a Hitachi 7100 transmission electron microscope.

Table 1
Implanted probe types and survival times.

Rat	Survival time (week)	Probe label	Electrode contacts	Shank size (μm × μm)	Probe base (assembly type)
NPR-01	1	D150C	–	150 × 100	Cable
NPR-02	1	D100C	–	100 × 100	Cable
NPR-03	1	E100P	+	100 × 100	Platform
NPR-04	2	D150C	–	150 × 100	Cable
NPR-05	2	D100C	–	100 × 100	Cable
NPR-06	2	E100P	+	100 × 100	Platform
NPR-07	4	D150C	–	150 × 100	Cable
NPR-08	4	D100C	–	100 × 100	Cable
NPR-09	4	E100P	+	100 × 100	Platform
NPR-10	12	D150C	–	150 × 100	Cable
NPR-11	12	D100C	–	100 × 100	Cable
NPR-12	12	E100P	+	100 × 100	Platform
NPR-13	8	D100C	–	100 × 100	Cable

2.4.2. Scanning electron microscopy

Explanted probes were removed from the fixative solution, thoroughly washed with distilled water, and dried at 40 °C for 24 h. They were covered with a thin gold layer by sputter deposition Emitech K550, and examined in a Jeol JSM-5800 scanning electron microscope.

2.5. Cell counting

In each animal, every 6th section, stained with the neuronal marker NeuN, was used to estimate cell loss around the probe tracks, within the entire depth of the neocortex. Sections containing probe tracks were examined by light microscope, and digitized with high resolution at 10× magnification. For manual analysis of NeuN positive cells, a grid of 100 μm × 100 μm squares was placed over the probe tracks, and neurons were counted in squares at a distance of 100, 200, 300 and 400 μm from the side of the probe tracks. For each distance and coating, cells were counted in 40–66 squares. Since neuronal density can vary in different neocortical layers, control areas were determined in each animal, for each coating. In all cases, two times 34 neighbouring squares ($n = 68$), covering the entire thickness of the cortex were chosen as control, located at least 600 μm from the probe tracks. Following standard stereological methods, cell bodies touching the top and left side of the grid were counted, while somata touching the bottom and right sides were excluded. Cell loss at a given distance for a given coating was determined as percentage of its control.

2.6. Blood vessel analysis

Two photos of the same size and magnification were used to determine the cross section area of blood vessels in superficial (layers II–III), and deep layers (V–VI) of the cortex. Both photos were taken from the same animal, around the same probe (NPR-10, Hya-DexM). Blood vessels were drawn and measured using the ImageJ program (Wayne Rasband, National Institutes of Health, USA).

2.7. Statistics

When data was normally distributed, one-way ANOVA on Ranks was used. Non-parametric Kruskal–Wallis ANOVA was used if a data set did not pass the normality test.

3. Results

The biocompatibility and the effect of different coatings on NeuroProbes silicon probes were investigated in the rat neocortex in vivo, at short and long terms. Three different types of probes were implanted into the dorsal neocortical areas of rats (see Section 2, Table 1, Fig. 1; Herwik et al., 2009). Glial reaction was described with qualitative analysis around the probe track, whereas neuronal numbers were quantified with manual stereological methods. Qualitative light microscopic analysis did not show notable differences among the cortices of rats implanted with different probe types.

3.1. Neuronal and glial cell distribution in the rat neocortex

The number and distribution of neuronal (Gould et al., 1999; Mullen et al., 1992) and astroglial cells (Eng and DeArmond, 1981; Kalman and Hajos, 1989) in control cortical areas at distances greater than 600 μm from probe tracks was comparable to previous descriptions.

NeuN-stained neural cell bodies were distributed throughout the rat neocortex. In layer I round, multipolar cells were present at low densities. Pyramidal shaped and multipolar neurons were observed in layers II–III and V–VI. Large pyramidal cells were especially evident in layer V, while in layer IV there were many small, round neuronal cell bodies but no large pyramidal cells (supplementary Fig. 1A). Glial fibrillary acidic protein (GFAP)-positive star-shaped astroglial cells with long processes were distributed homogeneously in the neocortex. The superficial layer I contained more positive elements, than other layers. Blood vessels were surrounded by strongly stained astroglial processes, throughout the neocortex (supplementary Fig. 1B).

3.2. Effect of bleeding during probe insertion

Inserted probes may puncture larger or smaller superficial blood vessels and so cause serious or minor bleeding. Altogether, we inserted $13 \times 5 = 65$ probes. Four of them hit large blood vessels resulting in severe bleeding that spread to all four shanks of the probe. In eight cases, smaller blood vessels were punctured and bleeding spread to one or two shanks. We examined the short or long term effect of bleeding on neuronal and glial cell densities. Signs of serious bleeding were visible at both 1 and 12 weeks after surgery. Tissue around the probe tracks was damaged and very few, if any, neurons or glial cells could be observed. A large hole was typically surrounded by dark, unspecific staining (result of the peroxidase reaction) that masked any stained neural or glial cell (Fig. 2). In some cases, but not always, patches with severe neuron loss were detected near damaged tissue (Fig. 2C), and in these regions glial cells were larger and darker than in the control case.

Dex reduces blood viscosity, erythrocyte aggregation and platelet adhesiveness resulting in a better lysis of clots (for reviews see Abir et al., 2004; Johnson and Barker, 1992). We therefore expected a reduced tissue reaction around Dex coated probes that had induced bleeding. Indeed, signs of bleeding were considerably less for the Dex coated E100P probe than for probes not coated with Dex at 4 weeks of survival. A lysed blood clot was outlined by a severe neuronal loss, but we did not detect either dark unspecific staining or damaged tissue (Fig. 2D) at light microscopic level.

Next, we attempted to estimate differences in blood vessel distribution between superficial and deep layers of rat neocortex (Fig. 3). We determined the cross sectional area of all blood vessels detected in photos of two NeuN-stained horizontal sections, one from layer II–III (supragranular layers), and the other from layer V–VI (infragranular layers). We found 274 blood vessels in a 2.55 mm^2 area in the supragranular region, with cross sectional areas ranging from 12 to 1467 μm^2, and a mean of 165 ± 186 μm^2 (mean ± st.dev.). In the infragranular layers, 188 blood vessels were present in the same area. The smallest and largest cross sectional areas were similar to that found in layers II–III: between 12 and 1273 μm^2. The mean cross sectional area was lower, 132 ± 169 μm^2. Both small and large blood vessels were more abundant in supragranular layers of the cortex, as shown by the frequency distribution analysis of the blood vessel cross sectional area (Fig. 3E). Blood vessels covered 1.77% and 0.97% of the total cortical area in supragranular and the infragranular layers, respectively (Fig. 3F). In summary, more and larger blood vessels are present in superficial layers, than in the deep layers of the neocortex.

3.3. Effect of different coatings on neuron survival

Different molecular surfaces might differentially influence neuronal and glial survival (for review see Cheung, 2007). We examined this question by quantifying neuron loss and by describing glial reaction around tracks of silicon probes with no coating or coated with different molecules. The following coatings were tested: hyaluronic acid (Hya), dextrane (Dex), dexamethasone (DexM) and

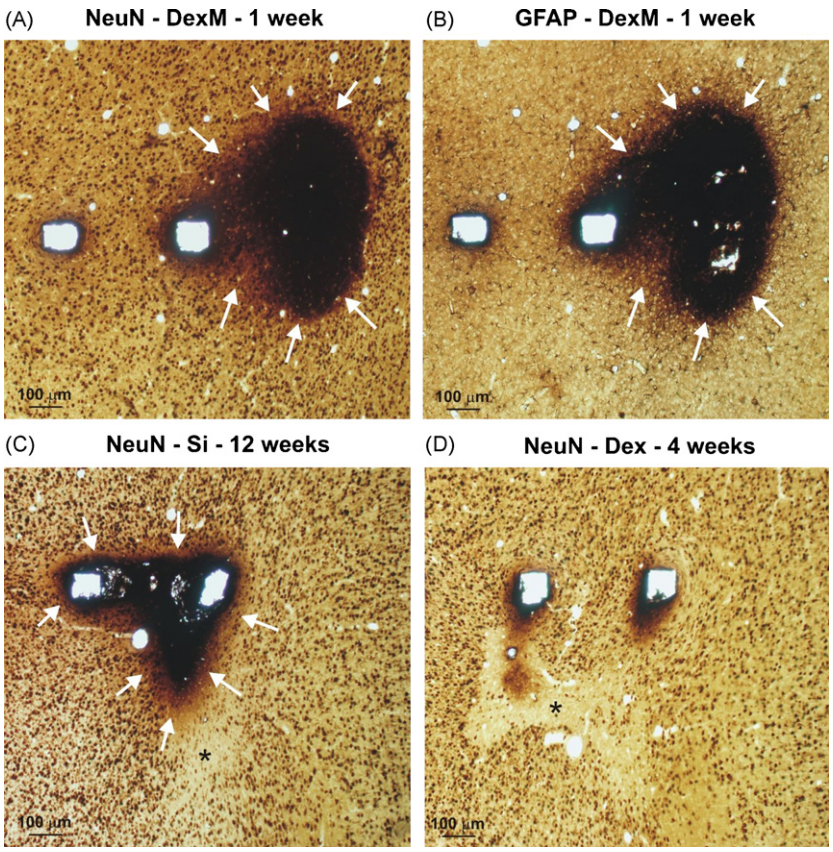

Fig. 2. Effects of bleeding during implantation. Signs of serious bleeding during implantation were evident at both at 1 week (A, B, arrows) and 12 weeks (C). The tissue was damaged around the probe tracks: a dark unspecific staining masked neuronal (A) and glial (B) immunostaining (DexM coated probe). In some cases, patches with severe neuron loss (asterisk) were observed near damaged tissue (C, Si probe) or next to the probe track without the signs of tissue damage (D, Dex coated probe).

a mixture of hyaluronic acid and dexamethasone (Hya/DexM). Rats were sacrificed after 1, 2, 4, 8 or 12 weeks after implantation (Table 1). Neurons were counted in squares of 100 μm × 100 μm around the probe tracks, and at distances of 200, 300 and 400 μm. All probe tracks where severe bleeding occurred during implantation were excluded from this part of the study. Control squares were defined in a line crossing the entire width of the cortex, at least 600 μm from the probe track (see Section 2) and these values were used as a control for cell numbers at sites closer to the probe.

At 1-week survival, we examined neuron numbers ($n = 21\,950$ cells in total) in a rat implanted with D150C type probes with different coatings. There was a considerable neuronal loss at distances within 100 μm of all tracks. The proportion of surviving neurons varied from 49.7 ± 2.8% to 76.0 ± 3.6%, compared to control with the highest neuronal death near Hya coated probes and the highest survival for the DexM coated probe. (Table 2, Fig. 4A, B). At distances of 200, 300 and 400 μm, neuronal loss was reduced with values of 80.4 ± 3.5% to 102.0 ± 3.3% of control at 400 μm from the track. The efficiency of the coatings in terms of optimal neuronal survival was the following: Hya < Dex < Si < Hya/DexM < DexM (Fig. 4D). At distance of 100 μm neuronal survival around DexM probe was significantly higher (Kruskal–Wallis ANOVA, $p < 0.001$) than around Hya, Dex and Si probes. Furthermore, Hya/DexM showed significantly larger neuron numbers than Hya (Table 2, Supplementary table* 1). Neuronal survival detected at 100 μm from the track of all probes was significantly reduced compared to that at 200, 300, 400 μm, and to control values (Table 3).

We also examined neuronal survival at 8 weeks after implantation. Neuronal densities ($n = 37\,805$ cells) were measured in a rat implanted with D100C probes. At distances of 100–400 μm from the probe track, neuronal loss was slight with densities at 100 μm ranging from 81.1 ± 4.0% to 92.2 ± 4.0% of control values, and between 93.8 ± 3.2% and 100.0 ± 2.9% at 400 μm (Table 4, Supplementary table* 1, Fig. 4C). While neuronal loss was reduced at this long survival period (and the D100C probe was different in size to the D150C probe used in the short survival period experiment), the efficiency of the coatings in terms of optimal neuronal survival followed a similar order: Hya < Dex < Si < Hya/DexM < DexM (Fig. 4D). At long term survival no statistical differences were found either between the different coatings or between the different locations (Kruskal–Wallis ANOVA, $p > 0.001$).

We obtained further data on how neuronal survival depends on time and varies with probe type, by measuring neuronal density after implantation of the same probe type at both short and long survival times (Fig. 4E). We counted neurons around E100P uncoated Si probes at 1, 2, 4 and 12 weeks survival ($n = 38\,773$ cells, Supplementary Fig. 2). At all time points, neuronal loss was largely restricted to distances less than 100 μm from the probe track (Table 5, Supplementary table* 1). Values for neuronal survival within this distance were lowest at 1 week (77.8 ± 2.3%). Two weeks after implantation these values were approximately 85% of control. Values at 1 week were significantly different from values at 12 weeks (Kruskal–Wallis ANOVA, $p < 0.001$). At distances of 200 to 400 μm, neuronal density was at least 90% of control values.

In summary, maximal neuronal loss occurs at 1 week after probe implantation and at distances less than 100 μm. The considerable neuron loss observed at this time point is reduced with time after implantation as neuronal densities return towards control values. Different probe coatings have an effect on neuronal survival at 1 week. However, this effect is reduced for longer delays after implantation.

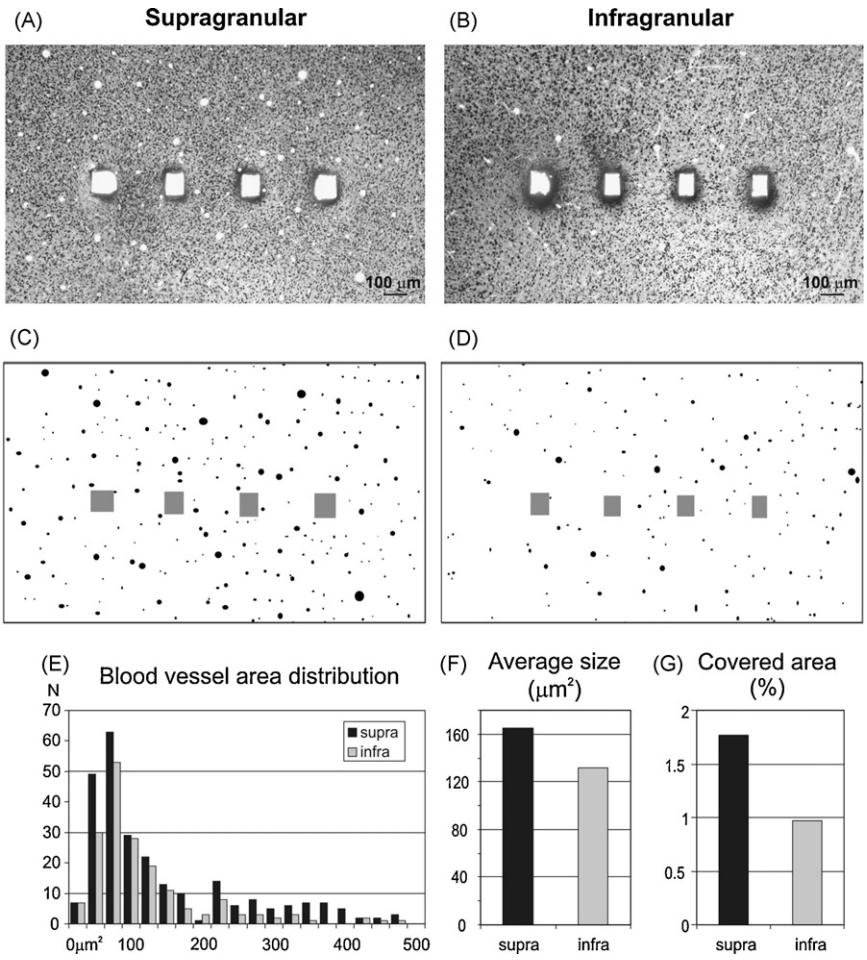

Fig. 3. Blood vessel distribution in rat neocortex. Photos (A, B) and drawings (C, D) show the cross section area of blood vessels in supragranular (A, C) and infragranular (B, D) layers of the cortex. Both small and large size blood vessels are more abundant in the supragranular layers (E); the average size (F) and the total area covered by the vessels (G) are also larger.

3.4. Glial reaction around the probes

Insertion of probes into the brain provokes a glial reaction (Fawcett and Asher, 1999; Polikov et al., 2005; Schwartz, 2004; Shain et al., 2003; Szarowski et al., 2003; Turner et al., 1999). Both glial cell density and the length and complexity of glial cell processes increase. Gliosis around probe tracks was investigated in qualitative analysis at light and electron microscopic levels of sections stained with the astroglial marker GFAP (Fig. 5, Supplementary Fig. 2B). Native silicon and all coatings of all three probe types were examined at all time points (1, 2, 4, 8 and 12 weeks).

In brains examined at 1 week after probe implantation, large, strongly stained "reactive astroglial cells" (Eng and DeArmond, 1981) were visible around the probe tracks, independent of the coating (Fig. 5A). At longer delays, glial cell numbers and shape returned to control levels even close to probe tracks and a dense glial scar was not observed visually, however we did not quantify our results statistically in the case of the glial observations. Light microscopic examination revealed no major influence visually, of probe size or coating on the gliotic response. Larger or smaller glial reactions were sometimes associated with different shanks of the same probe (Fig. 5B), possibly related to localized bleeding. If a major bleeding occurred during probe insertion, tissue was considerably damaged with large, dark glial cells surrounding the injured area.

In summary, slight gliosis was observed visually in all cases, but not a dense glial scar. Furthermore, we could not find any clearly visible correlation between the degree of the glial response and the coating of the probe. Higher glial reaction was

Table 2
Percentage of neurons at certain distances from the probe track, compared to control, at short term survival. Data are presented in mean ± S.E.M.

1 week	100 μm	200 μm	300 μm	400 μm
Si (n = 5396 cells)	62.3 ± 3.2%	88.5 ± 2.7%	88.3 ± 3.3%	92.6 ± 3.1%
Hya (n = 4744 cells)	49.7 ± 2.8%	73.3 ± 3.3%	82.7 ± 3.8%	87.1 ± 3.5%
Dex (n = 4124 cells)	55.0 ± 3.4%	76.2 ± 3.7%	81.5 ± 2.9%	80.4 ± 3.5%
DexM (n = 3798 cells)	76.0 ± 3.6%**	101.8 ± 3.2%	103.0 ± 3.2%	102.0 ± 3.3%
Hya/DexM (n = 3888 cells)	67.9 ± 3.4%*	90.2 ± 3.3%	101.3 ± 2.9%	101.4 ± 2.3%

DexM > Hya/DexM > Si > Dex > Hya. For statistical significances for the different locations around the same probe see Table 3.
** Significantly different from Si, Hya and Dex at 100 μm, $p < 0.001$.
* Significantly different from Hya at 100 μm, $p < 0.001$.

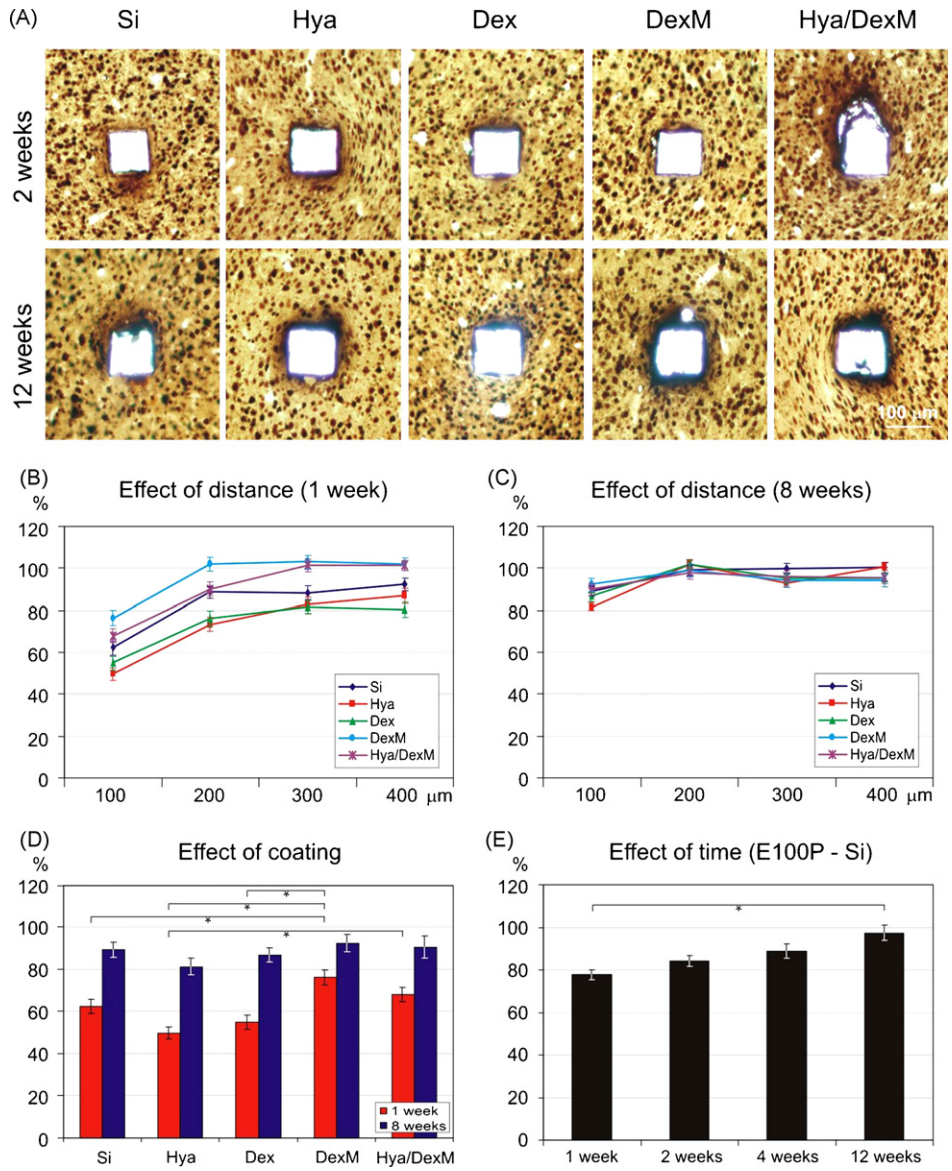

Fig. 4. Effect of coating on neuronal densities. Light micrographs show similar neuron numbers around tracks made by probes with different coatings (A). The most serious neuron loss was observed at 1-week survival, in the vicinity of the track (<100 μm), neuron numbers ranging from 49.7 ± 2.8% to 76.0 ± 3.6% compared to control (B). The neuronal density increases with distance from the track, and with survival time, reaching 81.1 ± 4.0% to 92.2 ± 4.0% at 8 weeks (C). Different coatings affect neuronal survival at 1-week survival, but effects become less significant at longer intervals. The efficacy of the different coatings Hya < Dex < Si < Hya/DexM < DexM is similar for short or long term survival (D). Neuronal loss observed at short term decreases with survival time (E). Error bars represent mean ± S.E.M. *$p < 0.001$.

usually seen at short survival time (1 week), or around bleedings.

3.5. Transmission electron microscopy of the probe tracks

Light microscopic examination showed statistically significant neuronal loss near probe tracks at 1 week after implantation. This cell loss decreases with distance from the track, and with survival time of the animal. Glial reactions judged by visual inspection were moderate, unless probe insertion provoked bleeding. We pursued the ultrastructural correlates of these changes in neurons and glial cells near probe tracks at the electron microscopic level. GFAP-stained sections were prepared from tissue close to the tracks of E100P Hya coated probes in animals at 1, 2, 4 and 12 weeks after implantation. In the animal at 1-week survival, one shank of the probe had provoked local bleeding whereas no signs of bleeding were detected at the other shanks (Figs. 5A, 6A and B). In the animal at 12 weeks survival, there was a high glial reaction around one shank but not around the others (Figs. 5B, 6C and D). Comparing various sections let us examine tissue preservation around the same probe type with the same coating, with or without bleeding and in the presence or absence of a strong glial reaction.

3.5.1. Neuronal cell bodies – tissue preservation

Healthy neuronal cell bodies must exist sufficiently close to implanted probes for any signal to be recorded. Light microscopy always showed numerous NeuN-stained neurons around the tracks of the probes. In the electron microscope, we examined the cell bodies of neurons located at distances less than 100 μm from probe tracks (Fig. 6). Neurons were distinguished from glial somata by the absence of the astroglial marker GFAP, by a light, homogenous nucleus, an electron-dense nucleolus and by a clear cytoplasmic structure and organelles. Immuno-positivity for GFAP was used to distinguish astrocytes while glial cell types including oligodendrocytes and microglia possess either very light cytoplasm with poor structure, or exhibit a dark, electron dense homogenous cyto-

Table 3
Statistical significances for the different locations around the different probes, at 1 week survival.

	100 μm	200 μm	300 μm	400 μm	Control
Si					
100 μm	–	*	*	*	*
200 μm	–	–	ns	ns	*
300 μm	–	–	–	ns	ns
400 μm	–	–	–	–	ns
Control	–	–	–	–	–
Hya					
100 μm	–	*	*	*	*
200 μm	–	–	ns	*	*
300 μm	–	–	–	ns	*
400 μm	–	–	–	–	*
Control	–	–	–	–	–
Dex					
100 μm	–	*	*	*	*
200 μm	–	–	ns	ns	*
300 μm	–	–	–	ns	*
400 μm	–	–	–	–	*
Control	–	–	–	–	–
DexM					
100 μm	–	*	*	*	*
200 μm	–	–	ns	ns	ns
300 μm	–	–	–	ns	ns
400 μm	–	–	–	–	ns
Control	–	–	–	–	–
Hya/DexM					
100 μm	–	*	*	*	*
200 μm	–	–	ns	*	ns
300 μm	–	–	–	ns	ns
400 μm	–	–	–	–	ns
Control	–	–	–	–	–

ns = not significant.
* $p < 0.05$.

Table 4
Percentage of neurons at certain distances from the probe track, compared to control, at long term survival. Data are presented in mean ± S.E.M.

8 weeks	100 μm	200 μm	300 μm	400 μm
Si (n = 8074 cells)	89.0 ± 3.6%	99.0 ± 3.4%	99.7 ± 3.5%	100.0 ± 2.9%
Hya (n = 8004 cells)	81.1 ± 4.0%	100.1 ± 2.9%	91.9 ± 4.2%	98.9 ± 3.6%
Dex (n = 8649 cells)	86.6 ± 3.4%	100.0 ± 3.5%	94.2 ± 3.5%	93.8 ± 3.2%
DexM (n = 6735 cells)	92.2 ± 4.0%	99.2 ± 3.6%	94.1 ± 4.5%	94.2 ± 4.0%
Hya/DexM (n = 6343 cells)	90.3 ± 5.4%	97.7 ± 4.4%	96.2 ± 4.4%	95.5 ± 3.7%

DexM > Hya/DexM > Si > Dex > Hya.

plasm and nucleus (Hama et al., 1994; King, 1968). Furthermore, the diameter of neuronal somata is typically 12–25 μm, whereas the diameter of glial cell is rather smaller at 5–10 μm.

At 1 week after probe implantation, we detected considerable tissue damage (Fig. 6A, B). Caverns, degenerating structures and incomplete membranes were observed around all shanks, including those where tissue damage was not apparent in the light microscope. Tissue injury extended to distances of 30–40 μm from tracks where no bleeding occurred (Supplementary Fig. 3A). In tissue around the track where bleeding was observed, signs of damage extended over a considerably larger region at distances up to 120–150 μm (Supplementary Fig. 3B). Glial cells and processes typically formed a layer of 5–10 μm thickness surrounding all probe tracks. There was no evidence for a dense glial scar, but rather glial and neuronal processes were intermingled. Neuronal cell bodies were detected at distances as close as 10 μm from tracks with no bleeding (Fig. 6A), and were not observed closer than ~50 μm when bleeding was detected during implantation (Fig. 6B).

Two weeks after probe implantation, tissue damage around the tracks was less than that detected at 1 week. Caverns were distributed in a patchy fashion, and the number of incomplete membranes and degenerating structures was reduced. The glial layer surrounding the track was unchanged. At 4 weeks after implantation, tissue preservation was good and few signs of injury

Table 5
Percentage of neurons at certain distances from the probe track, compared to control, at different time points, around E100P uncoated Si probes. Data are presented in mean ± S.E.M.

	100 μm	200 μm	300 μm	400 μm
1 week (n = 8576 cells)	77.8 ± 2.3%*	91.6 ± 2.9%	96.0 ± 2.7%	97.1 ± 3.1%
2 weeks (n = 10 557 cells)	84.3 ± 2.5%	93.2 ± 2.5%	89.9 ± 2.1%	89.6 ± 2.5%
4 weeks (n = 9965 cells)	86.5 ± 3.6%	99.9 ± 3.2%	99.3 ± 2.5%	100.0 ± 2.8%
12 weeks (n = 9675 cells)	85.1 ± 3.5%	98.7 ± 3.2%	97.4 ± 3.3%	100.0 ± 3.4%

* Significantly different from 12 weeks at 100 μm, $p < 0.001$.

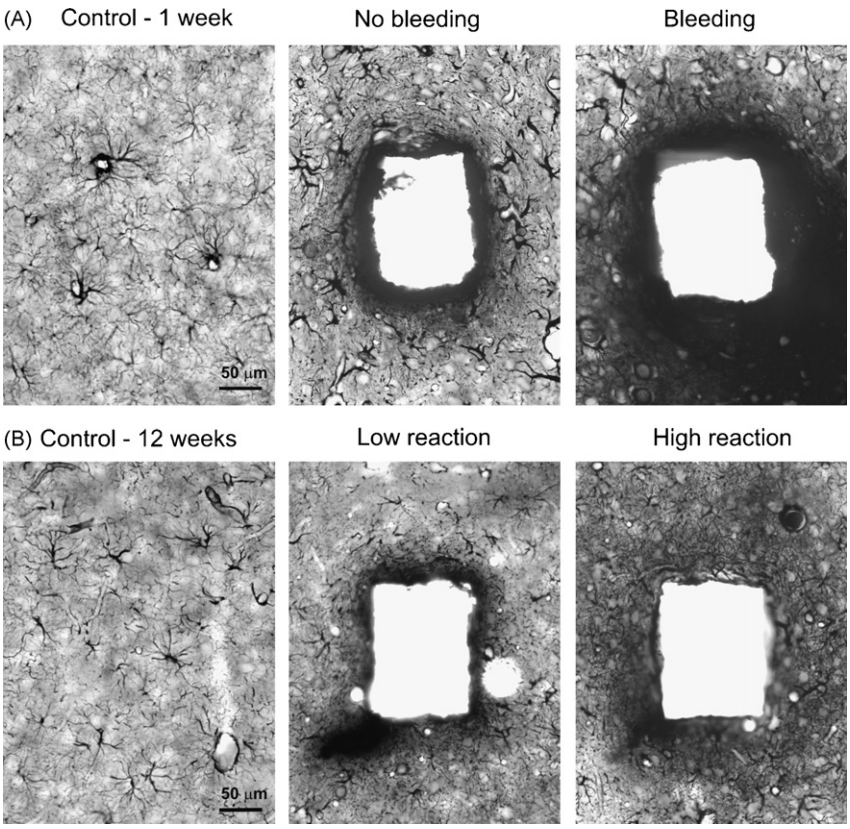

Fig. 5. Glial reaction around the probe tracks. In general, only moderate gliosis occurred at short (A, middle) and long (B, middle) term survival. Compared to control, larger and darkly stained reactive astroglial cells were visible around the tracks at 1-week survival (A, middle, right). At longer delays (12 weeks, B) glial cell numbers and shape returned to control levels (B, middle). In some cases, lower and higher glial reaction occurred around different shanks of the same probe (A, B), sometimes related to a serious bleeding (A, right).

were evident. Healthy neuronal cell bodies were present at distances as low as 10 μm from probe tracks. The glial margin of 5–10 μm thickness was retained. At one edge of one track, we detected an unusually thick and densely packed scar with a diameter of about 10–20 μm.

At 12 weeks survival, tissue preservation within distances of 100 μm from probe tracks was very good and difficult to distinguish from that at distances greater than 300 μm (Fig. 6C, D). We specifically compared tissue where a stronger or weaker glial reaction was observed in the light microscope. Little structural difference was evident although the number of GFAP-positive astroglial processes seemed to be higher in a 30–50 μm thick region around the track with high glial reaction. This network of astroglial processes did not form a dense glial scar according to our light microscopic visual inspection. Neuronal cell bodies were abundant around the tracks, sometimes at distances less than 10 μm (Fig. 6C, D).

3.5.2. Synapses

Electron microscopy also permits an estimate of the functional state of synaptic connections between neurons. We examined asymmetric, i.e. excitatory and symmetric i.e. inhibitory synapses close to tracks of implanted silicon probes. Numerous synapses were detected within 100 μm of the tracks at 1, 2, 4 and 12 weeks survival times, as well when bleeding or a strong glial reaction was detected (Fig. 7).

Damaged synapses were detected, mostly at 1 or 2 weeks survival times and their extent was closely related to the degree of tissue damage. Typically, the outer membranes of pre- and postsynaptic elements were discontinuous, whereas the synaptic cleft was unaffected as were synaptic vesicles (Fig. 7A, B). When tissue damage was considerable, asymmetrical (excitatory) synapses seemed to predominate over symmetrical (inhibitory) synapses. In well preserved cortical areas numerous asymmetrical and symmetrical synapses were detected. Synapses of both types were detected close to probe tracks, sometimes as close as 5 μm when tissue damage was only moderate or very slight (Fig. 7C, D).

3.6. Scanning electron microscopy of the explanted probes

Brain tissue exhibits a glial reaction, including the liberation of inflammatory molecules, in response to injury (Fawcett and Asher, 1999; Polikov et al., 2005). Furthermore, extracellular compartments even in undamaged brain may contain water-soluble elements that affect electrode surfaces. To obtain a qualitative insight into possible changes at the electrode surface without strict statistical power, we examined explanted probes with scanning electron microscopy to see how the surface of the silicon was altered after spending short and long periods in the rat neocortex (E100P probes, 1, 2, 4 and 12 weeks of survival, all different coatings).

As in previous works (Biran et al., 2005; Turner et al., 1999), all examined explanted probes were partly covered by tissue residues and/or by a cell layer (Fig. 8A). We expected obvious differences in the probe surface coverage, due to different attributes of biocoating molecules: more tissue residues/cells on the good neural adhesion surface Hya coated probe, than on the others. However we detected no clearly visible relation between the covered probe surface and the coating.

Cells with different morphologies remained in contact with the surface of explanted probes. They were typically small, flat and round cells forming a densely packed, continuous layer (Fig. 8B).

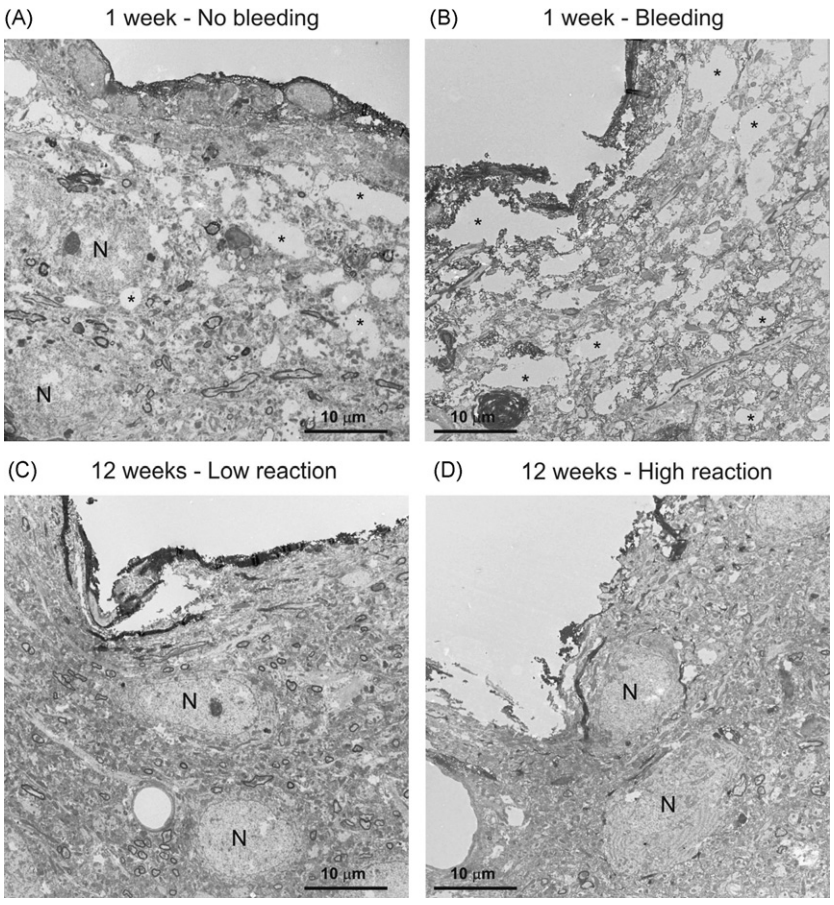

Fig. 6. Transmission electron micrographs of the probe tracks shown in Fig. 5 at 1 week (A, B) and 12 weeks (C, D) survival. Large caverns (asterisks) and damaged membranes were found next to the tracks at 1 week survival (A, B), whereas the tissue was not damaged at 12 weeks (C, D). In all cases, neuronal cell bodies (N on A, C, D) were found within 100 μm from the border of the probe tracks. Numerous neurons were observed at less than 20 μm from the track.

Less frequently, we detected large multipolar amoeboid cells, similar to fibrous astrocytes (Fig. 8C), as well as fusiform glial-like cells (Fig. 8D) and in some cases red blood cells (not shown) were present. Pt electrode contacts were also covered by tissue residue to different extents from no to total coverage (Fig. 8E, F).

4. Discussion

Implanted recording and stimulation microprobes are indispensable tools for research on the function of the intact brain, but their utility depends on biocompatibility and long term viability. Silicon-based surfaces are known to be highly biocompatible (Rutten, 2002). However, acute and chronic inflammatory processes seem likely to affect the surrounding neural tissue (for review see Polikov et al., 2005).

In this study we explored the biocompatibility of NeuroProbes silicon probes, and also asked how the brain environment modifies the probe surface. We showed that major bleeding during the implantation procedure can result in serious tissue damage. Even without large bleeding, implantation induces considerable short term neuronal loss. However, neuronal density close to the probe recovers to ~90% of control values at 2–4 weeks after implantation. Some gliosis occurs around probes implanted for short and long periods. Coating the silicon surface with different bioactive molecules has only a minor impact on neuronal loss. DexM coated probes gave the most promising results. The surface of recovered probes was usually partly covered by tissue residue containing diverse cell types.

4.1. Probe implantation

Probe insertion is the first step in long term brain recording and stimulation. The best recordings are achieved from a neural tissue that is as intact as possible. Several approaches have been tried by different research groups to achieve the best insertion procedure. Similar to our group (Cash et al., 2009; Fabo et al., 2008; Keller et al., 2009; Lakatos et al., 2008; Ulbert et al., 2001, 2004a,b; Wang et al., 2005), many researchers insert the probes by hand (Liu et al., 1999; Stensaas and Stensaas, 1976; Szarowski et al., 2003; Williams et al., 1999; Yuen and Agnew, 1995), whereas others use microdrives (Csicsvari et al., 2003; Maynard et al., 2000; Nicolelis et al., 2003). Insertion speed might also considerably differ, from slow (100 μm/s, Nicolelis et al., 2003) to rapid (8.3 m/s, Maynard et al., 2000) insertion. In addition, a more recent report (Biran et al., 2005) gives an interesting insight to the comparison of hand versus mechanically guided implantation. Biran et al. implanted un-tethered probes by hand and tethered ones with a microdrive. The tissue reaction outcome was favorable for the un-tethered, hand implanted probes. In conclusion, hand implantation may represent a worst case scenario, but it is still a viable and reliable method as indicated by several reports (for review see Polikov et al., 2005).

4.2. Effects of bleeding

As it was demonstrated in previous studies (Stensaas and Stensaas, 1976; Turner et al., 1999) we also showed that if a blood vessel is punctured during probe implantation and seri-

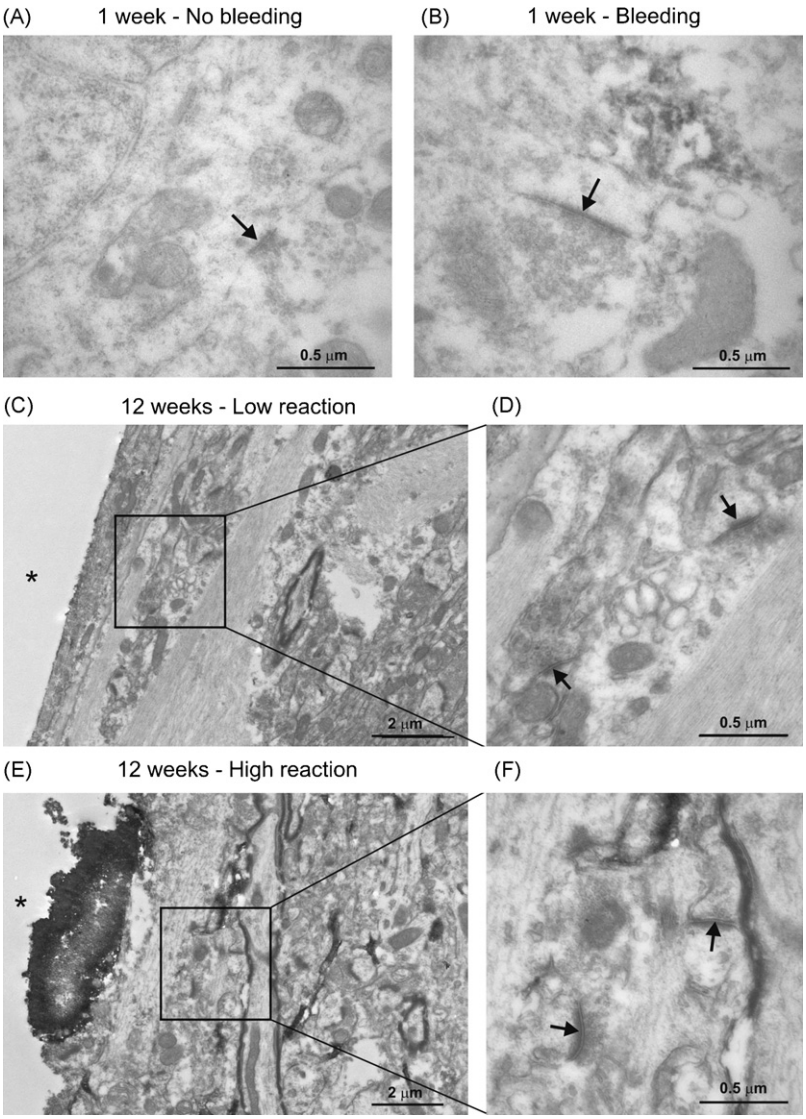

Fig. 7. Transmission electron micrographs show synapses found close to the probe tracks at 1 week (A, B) and 12 weeks (C–F) survival. Membranes of the pre- and postsynaptic elements were discontinuous when the tissue was damaged around the probes (A, B), but the synaptic cleft seemed to be preserved (arrows). Numerous synapses were found in the close vicinity of the track, at both with low (C, D) and high (E, F) glial reaction. Squares on C and E are enlarged on D and F, respectively. Asterisk indicates part of the track.

ous bleeding results, surrounding tissue is considerably damaged. Although neuronal cell bodies were observed in damaged tissue within 100 μm from the track, electron microscopy showed that their membranes were disrupted, and large cavities were present throughout damaged tissue. Electrode contacts located in highly damaged tissue probably generate low quality signals since neurons with incomplete membranes seem likely to be functionally compromised. This hypothesis should be tested with functional probes.

Our work revealed larger and more numerous blood vessels in upper than in deep layers of rat neocortex. Bleeding due to vessel disruption is therefore most likely near the cortical surface. However, the largest vessels typically run on the cortical surface and so can be visually avoided when the skull is open. Puncture of large vessels during implantation leads to severe bleeding and widespread neuronal death. In this experimental series, large blood vessels were penetrated in only 4 out of 65 cases (6.2%). In previous studies (Devor et al., 2007, 2008), we imaged the vasculature of the superficial 300 μm of the rat cortex, and found a very dense network of vessels. It seems that there is a limited chance to preserve all the fine vessels without precisely imaging the vasculature and specifically plan the probe implantation trajectory. Our blood vessel quantification results further strengthen these observations, and indicate that the chance to avoid bleeding by "blind" implantation is limited.

We used some probes coated with the antithrombotic agent Dex, in an attempt to reduce tissue damage during probe implantation. Considerable bleeding occurred while one such Dex-coated probe was implanted and in this case signs of tissue damage seemed to be reduced. The clot was lysed and characteristic unspecific dark staining disappeared, but neuronal loss was still evident. One case does not permit firm conclusions, but Dex coating may assist clot lysis and reduce tissue response, even though it clearly does not prevent the associated neuronal death.

4.3. Effects of coating

4.3.1. Neuron numbers

Probe surfaces were coated with Hya, Dex, DexM or Hya/DexM, in an attempt to diminish acute and chronic inflammatory and glial responses. Hya, a component of the extracellular matrix, has been

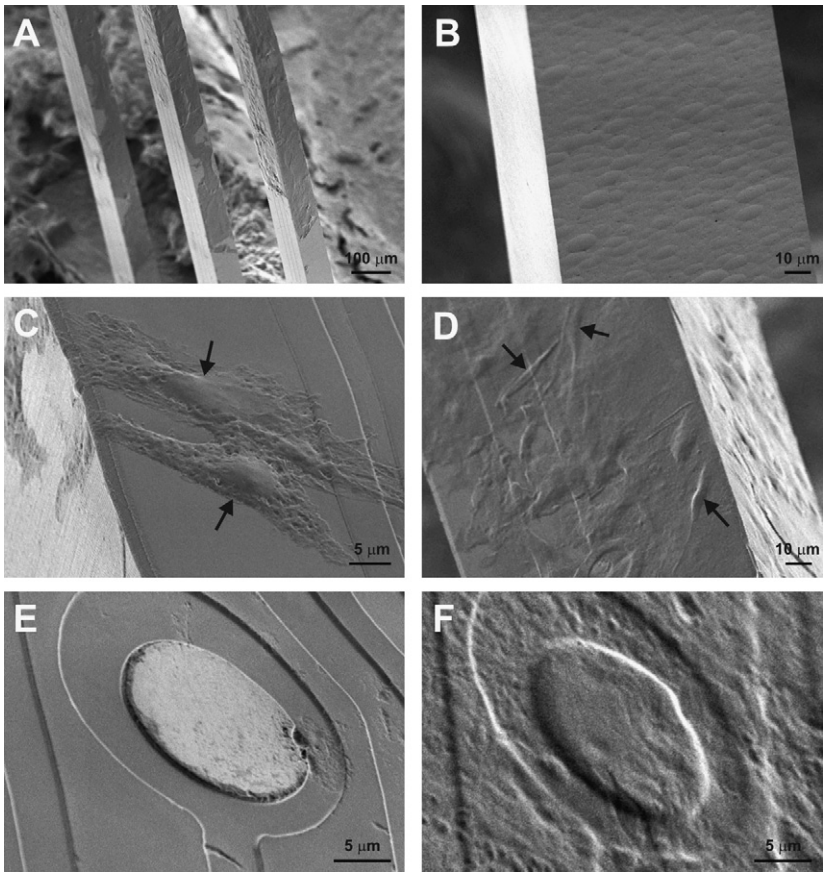

Fig. 8. Scanning electron micrographs of explanted probes. Low magnification photo shows the tissue residue partly covering the probe surface (A). Usually activated microglia-like, small round cells formed a densely packed layer on the explanted probes (B). Astroglia-like large (C), and small fusiform cells (D) were also observed. In some cases, electrode contacts were free of tissue residue (E), but totally covered contacts were also observed (F).

shown to reduce glial scar formation in rat neocortex (Lin et al., 2009). Dex is an antithrombotic agent helping clot lysis (for reviews see Abir et al., 2004; Johnson and Barker, 1992), whereas DexM is an agent decreasing inflammatory response (Shain et al., 2003; Spataro et al., 2005; Zhong and Bellamkonda, 2007; Zhong et al., 2005). Since all coating molecules are known to reduce tissue reaction, we expected better neuronal survival around coated probes. However only DexM coating had satisfactory effects on neuronal survival, while proportions of surviving neurons with Dex and Hya coated probes were lower than when uncoated Si probes were used (DexM > Hya/DexM > Si > Dex > Hya was the rank order of coating efficacy). As in previous work (Biran et al., 2005), cell loss was restricted to distances of less than 100 μm from the probe surface. Neuronal loss within such a radius may severely compromise spike records since different types of probes seem to record action potentials only within a radius of 80–100 μm (Buzsaki, 2004; Cohen and Miles, 2000; Wang et al., 2005).

Numbers of neurons were considerably decreased (49.7 ± 2.8% to 76.0 ± 3.6% of neurons surviving compared to control regions) close to all probes during the acute inflammatory response at 1 week after implantation. Interestingly, cell density was largely restored after 2 months (81.1 ± 4.0% to 92.2 ± 4.0%). This raises the question how neuronal density increases with time. Neurogenesis in the adult rat neocortex is debated, but the consensus is that newly generated cells are glial elements (for reviews see Gould, 2007; Rakic, 2002). Possibly neurons migrate back towards the probes when the acute oedema decreases. Transmission electron microscopy showed caverns of variable size surrounding tracks at 1 week, within a radius of about ~30 μm with no bleeding and in a radius of ~150 μm with extensive bleeding. These caverns and incomplete membranes presumably result from mechanical damage and the inflammatory reaction to probe insertion (Cheung, 2007). Damaged structures are presumably removed over time (Streit, 1996; Streit et al., 1999), permitting surviving neurons to migrate into and fill the volume around the probe.

Our analysis of the pattern of neuronal loss also suggested that surface coating of silicon probes affects neuronal density in the acute but not the chronic phase of inflammatory processes, and only if bleeding during probe implantation is avoided. Conceivably bioactive coating molecules, may have been degraded or destroyed by activated microglial cells or macrophages (Streit, 1996; Streit et al., 1999).

4.3.2. Glial response

Reactive tissue tends to engulf objects implanted in the brain (Agnew et al., 1986; Edell et al., 1992; McCreery et al., 1997; Schultz and Willey, 1976; Szarowski et al., 2003; Turner et al., 1999). This encapsulation response includes the formation of a glial scar. Such a scar could tend to insulate electrode contacts from neurons, and degrade unit recording quality (Roitbak and Sykova, 1999; Schultz and Willey, 1976; Turner et al., 1999). In contrast to this pessimistic scenario, as others in a previous study (Hoogerwerf and Wise, 1994), we detected only a moderate gliosis around all probes at all time points, independent of the presence or absence of any coating. Large and more strongly stained reactive astroglial cells (Polikov et al., 2005) were observed at the borders of injured areas both during acute inflammation at 1 week and after site specific bleeding. However while glial processes clearly surrounded probe tracks, the formation of a dense glial scar was not evident in transmission electron microscopy. Electron microscopy also revealed

neuronal somata (cf. Fig. 6), dendrites, and synapses (cf. Fig. 7) at distances as close as 10 μm to probe tracks. Two factors might account for the absence of a notable glial scar. First, the probes used were non-functional silicon probes with no connecting cable fixed to the skull with a reduced possibility of movement that might aggravate mechanical injury (Biran et al., 2005). Second, we assured probe sterility by storage in ethanol until surgery and transfer to distilled water a day before use. Such enhanced sterility standards may reduce astroglial encapsulation of implanted probes.

4.4. Surface of the probes

We examined the surface of probes implanted in the brain for different time periods by scanning electron microscopy. Cells of diverse morphologies were detected in the tissue residue covering explanted probes. Since Hya is an extracellular matrix element, we assumed it might provide an adhesive surface to attract neurons and glial cells. However, Hya coated probes were not covered by a more profuse tissue residue than uncoated probes. Furthermore, as suggested (Szarowski et al., 2003), the quantity of tissue residue was uncorrelated with the duration of the implantation. We note however, that the quantity of tissue residue and the number of cells visible on the surface of the explanted probes might also depend on the probe removal method. Our probes were removed manually after perfusion. It is possible that different removal procedures may provide more tissue residue on the probe surface, but a standardized removal method has yet to be established to effectively compare tissue residue on differently treated probes.

Cells with different anatomical features were distinguished on the probe surface (Fig. 8). The small, flat, round cells forming a densely packed continuous layer probably correspond to activated microglia (Biran et al., 2005). The large multipolar, amoeboid cells resemble fibrous astrocytes (Spataro et al., 2005; Wadhwa et al., 2006) or fibroblasts (Todaro and Green, 1963), whereas the fusiform cells may correspond to either glial cells (Spataro et al., 2005) or macrophages (Biran et al., 2005). Specific staining techniques are needed to identify definitively the cell types that attach to probes.

5. Conclusions

Biocompatibility and long term viability are crucial questions for chronic applications of implanted devices. Our data shows that the silicon-based microprobes developed in the framework of the NeuroProbes project are highly biocompatible. Neuronal loss around the probes was evident at 1 week after implantation within distances of 100 μm from the probe track. However, it was considerably reduced with time, with neuronal densities returning to 90% of control levels at 2–4 weeks after implantation. Disruption of major blood vessels resulted in considerable tissue damage, destroying most neurons over an area with a radius of several 100 μm. Both light and electron microscopic analyses showed a moderate gliosis around the probes in cases of minor or no bleeding, but a dense glial scar did not develop. We coated the silicon surface of the probes with different bioactive molecules in order to diminish tissue reactions. Coatings had minor effects on neuronal survival with only DexM showing an improvement as compared to native silicon probes. Our study suggests that avoiding blood vessel disruption during implantation may be a very important factor in preserving neuronal density around implanted devices.

Acknowledgements

We wish to thank Ms K. Iványi, K. Lengyel, E. Simon, K. Faddi, Mr P. Kottra and Gy. Goda for excellent technical assistance. This study was supported by the Hungarian Government OTKA K81357 grant and Bolyai János Research Fellowship grant and European Union NeuroProbes EU IP IST-027017 grant.

Appendix A. Supplementary data

Supplementary data associated with this article can be found, in the online version, at doi:10.1016/j.jneumeth.2010.04.009.

References

Aarts AAA, Neves HP, Puers RP, Van Hoof C. An interconnect for out-of-plane assembled biomedical probe arrays. J Micromech Microeng 2008;18:064004–10.
Abir F, Barkhordarian S, Sumpio BE. Efficacy of dextran solutions in vascular surgery. Vasc Endovascular Surg 2004;38:483–91.
Agnew WF, Yuen TG, McCreery DB, Bullara LA. Histopathologic evaluation of prolonged intracortical electrical stimulation. Exp Neurol 1986;92:162–85.
Biran R, Martin DC, Tresco PA. Neuronal cell loss accompanies the brain tissue response to chronically implanted silicon microelectrode arrays. Exp Neurol 2005;195:115–26.
Buzsaki G. Large-scale recording of neuronal ensembles. Nat Neurosci 2004;7:446–51.
Cash SS, Halgren E, Dehghani N, Rossetti AO, Thesen T, Wang C, et al. The human K-complex represents an isolated cortical down-state. Science 2009;324:1084–7.
Cheung KC. Implantable microscale neural interfaces. Biomed Microdevices 2007;9:923–38.
Cohen I, Miles R. Contributions of intrinsic and synaptic activities to the generation of neuronal discharges in in vitro hippocampus. J Physiol 2000;524(Pt 2):485–502.
Csicsvari J, Henze DA, Jamieson B, Harris KD, Sirota A, Bartho P, et al. Massively parallel recording of unit and local field potentials with silicon-based electrodes. J Neurophysiol 2003;90:1314–23.
Devor A, Hillman EM, Tian P, Waeber C, Teng IC, Ruvinskaya L, et al. Stimulus-induced changes in blood flow and 2-deoxyglucose uptake dissociate in ipsilateral somatosensory cortex. J Neurosci 2008;28:14347–57.
Devor A, Tian P, Nishimura N, Teng IC, Hillman EM, Narayanan SN, et al. Suppressed neuronal activity and concurrent arteriolar vasoconstriction may explain negative blood oxygenation level-dependent signal. J Neurosci 2007;27:4452–9.
Edell DJ, Toi VV, McNeil VM, Clark LD. Factors influencing the biocompatibility of insertable silicon microshafts in cerebral cortex. IEEE Trans Biomed Eng 1992;39:635–43.
Eng LF, DeArmond SJ. Glial fibrillary acidic (GFA) protein immunocytochemistry in development and neuropathology. Prog Clin Biol Res 1981;59A:65–79.
Fabo D, Magloczky Z, Wittner L, Pek A, Eross L, Czirjak S, et al. Properties of in vivo interictal spike generation in the human subiculum. Brain 2008;131:485–99.
Fawcett JW, Asher RA. The glial scar and central nervous system repair. Brain Res Bull 1999;49:377–91.
Fraser JR, Laurent TC, Laurent UB. Hyaluronan: its nature, distribution, functions and turnover. J Intern Med 1997;242:27–33.
Frey O, van der Wal P, de Rooij N, Koudelka-Hep M. Development and characterization of choline and glutamate biosensor integrated on silicon microprobes for in-vivo monitoring. In: EMBC Proc. 29th Annu. Int. Conf. IEEE Eng. in Med. and Biol. Soc.; 2007. p. 6039–42.
Gallus AS, Hirsh J. Antithrombotic drugs: part II. Drugs 1976;12:132–57.
Gould E. How widespread is adult neurogenesis in mammals? Nat Rev Neurosci 2007;8:481–8.
Gould E, Reeves AJ, Graziano MS, Gross CG. Neurogenesis in the neocortex of adult primates. Science 1999;286:548–52.
Hama K, Arii T, Kosaka T. Three-dimensional organization of neuronal and glial processes: high voltage electron microscopy. Microsc Res Tech 1994;29:357–67.
Herwik S, Kisban S, Arts AA, Seidl K, Girardeau G, Benchenane K, et al. Fabrication technology for silicon-based microprobe arrays used in acute and sub-chronic neural recording. J Micromech Microeng 2009;19, 074008 (11 pp.).
Hoogerwerf AC, Wise KD. A three-dimensional microelectrode array for chronic neural recording. IEEE Trans Biomed Eng 1994;41:1136–46.
Johnson PC, Barker JH. Thrombosis and antithrombotic therapy in microvascular surgery. Clin Plast Surg 1992;19:799–807.
Jones CI, Payne DA, Hayes PD, Naylor AR, Bell PR, Thompson MM, et al. The antithrombotic effect of dextran-40 in man is due to enhanced fibrinolysis in vivo. J Vasc Surg 2008;48:715–22.
Kaal EC, Vecht CJ. The management of brain edema in brain tumors. Curr Opin Oncol 2004;16:593–600.
Kalman M, Hajos F. Distribution of glial fibrillary acidic protein (GFAP)-immunoreactive astrocytes in the rat brain. I. Forebrain. Exp Brain Res 1989;78:147–63.
Keller CJ, Cash SS, Narayanan S, Wang C, Kuzniecky R, Carlson C, et al. Intracranial microprobe for evaluating neuro-hemodynamic coupling in unanesthetized human neocortex. J Neurosci Methods 2009;179:208–18.
King JS. A light and electron microscopic study of perineuronal glial cells and processes in the rabbit neccortex. Anat Rec 1968;161:111–23.
Koehler PJ. Use of corticosteroids in neuro-oncology. Anticancer Drugs 1995;6:19–33.
Lakatos P, Karmos G, Mehta AD, Ulbert I, Schroeder CE. Entrainment of neuronal oscillations as a mechanism of attentional selection. Science 2008;320:110–3.

Ledung G, Bergkvist M, Quist AP, Gelius U, Carlsson J, Oscarsson S. A novel method for preparation of disulfides on silicon. Langmuir 2001;17:6056–8.
Lin CM, Lin JW, Chen YC, Shen HH, Wei L, Yeh YS, et al. Hyaluronic acid inhibits the glial scar formation after brain damage with tissue loss in rats. Surg Neurol 2009;72:50–4.
Liu X, McCreery DB, Carter RR, Bullara LA, Yuen TG, Agnew WF. Stability of the interface between neural tissue and chronically implanted intracortical microelectrodes. IEEE Trans Rehabil Eng 1999;7:315–26.
Massia SP, Stark J, Letbetter DS. Surface-immobilized dextran limits cell adhesion and spreading. Biomaterials 2000;21:2253–61.
Maynard EM, Fernandez E, Normann RA. A technique to prevent dural adhesions to chronically implanted microelectrode arrays. J Neurosci Methods 2000;97:93–101.
McCreery DB, Yuen TG, Agnew WF, Bullara LA. A characterization of the effects on neuronal excitability due to prolonged microstimulation with chronically implanted microelectrodes. IEEE Trans Biomed Eng 1997;44:931–9.
Merrill DR, Bikson M, Jefferys JG. Electrical stimulation of excitable tissue: design of efficacious and safe protocols. J Neurosci Methods 2005;141:171–98.
Mullen RJ, Buck CR, Smith AM. NeuN, a neuronal specific nuclear protein in vertebrates. Development 1992;116:201–11.
Neves HP, Orban GA, Koudelka-Hep M, Ruther P. Development of multifunctional probe arrays for cerebral applications. In: Proc. 3rd Int. IEEE EMBS Conf. on Neural Eng.; 2007. p. 104–9.
Nicolelis MA, Dimitrov D, Carmena JM, Crist R, Lehew G, Kralik JD, et al. Chronic, multisite, multielectrode recordings in macaque monkeys. Proc Natl Acad Sci USA 2003;100:11041–6.
Pasqui D, Atrei A, Barbucci R. A novel strategy to obtain a hyaluronan monolayer on solid substrates. Biomacromolecules 2007;8:3531–9.
Paxinos G, Watson C. The rat brain in stereotaxic coordinates. 4th ed. San Diego, CA, USA: Academic Press; 1998.
Polikov VS, Tresco PA, Reichert WM. Response of brain tissue to chronically implanted neural electrodes. J Neurosci Methods 2005;148:1–18.
Pouyani T, Prestwich GD. Functionalized derivatives of hyaluronic acid oligosaccharides: drug carriers and novel biomaterials. Bioconjug Chem 1994;5:339–47.
Rakic P. Neurogenesis in adult primates. Prog Brain Res 2002;138:3–14.
Roitbak T, Sykova E. Diffusion barriers evoked in the rat cortex by reactive astrogliosis. Glia 1999;28:40–8.
Ruther P, Arts A, Frey O, Herwik S, Kisban S, Seidl K, et al. The NeuroProbes Project - Multifunctional probe arrays for neural recording and stimulation. In: Proc. Annual Conference of the IFESS; 2008. p. 238–40.
Rutten WL. Selective electrical interfaces with the nervous system. Annu Rev Biomed Eng 2002;4:407–52.
Schultz RL, Willey TJ. The ultrastructure of the sheath around chronically implanted electrodes in brain. J Neurocytol 1976;5:621–42.
Schwartz AB. Cortical neural prosthetics. Annu Rev Neurosci 2004;27:487–507.
Shain W, Spataro L, Dilgen J, Haverstick K, Retterer S, Isaacson M, et al. Controlling cellular reactive responses around neural prosthetic devices using peripheral and local intervention strategies. IEEE Trans Neural Syst Rehabil Eng 2003;11:186–8.
Spataro L, Dilgen J, Retterer S, Spence AJ, Isaacson M, Turner JN, et al. Dexamethasone treatment reduces astroglia responses to inserted neuroprosthetic devices in rat neocortex. Exp Neurol 2005;194:289–300.
Spieth S, Schumacher A, Seidl K, Hiltmann K, Haeberle S, Ruther P, et al. Robust microprobe systems for simultaneous neural recording and drug delivery. In: IFMBE Proc. Europ. Biomed. Eng. Congress; 2008. p. 2426–30.
Stensaas SS, Stensaas LJ. The reaction of the cerebral cortex to chronically implanted plastic needles. Acta Neuropathol 1976;35:187–203.
Streit WJ. The role of microglia in brain injury. Neurotoxicology 1996;17:671–8.
Streit WJ, Walter SA, Pennell NA. Reactive microgliosis. Prog Neurobiol 1999;57:563–81.
Szarowski DH, Andersen MD, Retterer S, Spence AJ, Isaacson M, Craighead HG, et al. Brain responses to micro-machined silicon devices. Brain Res 2003;983:23–35.
Todaro GJ, Green H. Quantitative studies of the growth of mouse embryo cells in culture and their development into established lines. J Cell Biol 1963;17:299–313.
Turner JN, Shain W, Szarowski DH, Andersen M, Martins S, Isaacson M, et al. Cerebral astrocyte response to micromachined silicon implants. Exp Neurol 1999;156:33–49.
Twycross R. The risks and benefits of corticosteroids in advanced cancer. Drug Saf 1994;11:163–78.
Ulbert I, Halgren E, Heit G, Karmos G. Multiple microelectrode-recording system for human intracortical applications. J Neurosci Methods 2001;106:69–79.
Ulbert I, Heit G, Madsen J, Karmos G, Halgren E. Laminar analysis of human neocortical interictal spike generation and propagation: current source density and multiunit analysis in vivo. Epilepsia 2004a;45(Suppl. 4):48–56.
Ulbert I, Magloczky Z, Eross L, Czirjak S, Vajda J, Bognar L, et al. In vivo laminar electrophysiology co-registered with histology in the hippocampus of patients with temporal lobe epilepsy. Exp Neurol 2004b;187:310–8.
Wadhwa R, Lagenaur CF, Cui XT. Electrochemically controlled release of dexamethasone from conducting polymer polypyrrole coated electrode. J Control Release 2006;110:531–41.
Wang C, Ulbert I, Schomer DL, Marinkovic K, Halgren E. Responses of human anterior cingulate cortex microdomains to error detection, conflict monitoring, stimulus-response mapping, familiarity, and orienting. J Neurosci 2005;25:604–13.
Williams JC, Rennaker RL, Kipke DR. Long-term neural recording characteristics of wire microelectrode arrays implanted in cerebral cortex. Brain Res Brain Res Protoc 1999;4:303–13.
Yuen TG, Agnew WF. Histological evaluation of polyesterimide-insulated gold wires in brain. Biomaterials 1995;16:951–6.
Zhong Y, Bellamkonda RV. Dexamethasone-coated neural probes elicit attenuated inflammatory response and neuronal loss compared to uncoated neural probes. Brain Res 2007;1148:15–27.
Zhong Y, McConnell GC, Ross JD, DeWeerth SP, Bellamkonda RV. A novel dexamethasone-releasing, anti-inflammatory coating for neural implants. In: 2nd International IEEE EMBS Conference on Neural Engineering; 2005. p. v–viii.